PROCEEDINGS OF SCIENCE

# Investigating Muon Production from Initial Hadronic Interactions in Cosmic Air Showers with a One-ton Scintillator Detector at CJPL

**Xinshun Zhang**[a,b,*] **and Jinjing Li**[c,d,e]

[a] *Department of Engineering Physics & Center for High Energy Physics, Tsinghua University, Beijing 100084, China*

[b] *Key Laboratory of Particle & Radiation Imaging (Tsinghua University), Ministry of Education, China*

[c] *School of Physics & Electronics, Hunan University, Changsha 410082, China*

[d] *School for Theoretical Physics, Hunan University, Changsha 410082, China*

[e] *Hunan Provincial Key Laboratory of High-Energy Scale Physics and Applications, Changsha 410082, China*

*E-mail:* zxs22@mails.tsinghua.edu.cn, lijinjing@hnu.edu.cn

Over the past decade, ground-based array experiments have reported a notable deficit in simulated muons from extensive air showers (EAS) induced by high-energy cosmic rays, compared with experimental observations. This discrepancy is known as the *muon puzzle*. In this work, we present the first study of this issue at the China Jinping Underground Laboratory (CJPL), where a 2400-m vertical rock overburden restricts muons to energies above 3 TeV, corresponding to an average primary cosmic-ray energy of about 0.4 PeV. This provides a clean window for probing the initial stages of EAS development. Using data collected over 1338.6 live days with the 1-ton prototype of the Jinping Neutrino Experiment, together with a GEANT4-based flux simulation framework, we perform a direct comparison between the measurement and predictions. Our results show that the observed muon flux is about 40% higher than post-LHC model expectations, offering new constraints for resolving the muon puzzle. These findings underscore the potential of deep underground environments for future high-energy cosmic-ray research.

39th International Cosmic Ray Conference (ICRC2025)
15–24 July 2025
Geneva, Switzerland

ICRC 2025
The Astroparticle Physics Conference
Geneva July 15-24, 2025

*Speaker





PoS(ICRC2025)452

## 1. Introduction

When high-energy cosmic rays from space arrive at the Earth, they collide with the atmosphere and generate extensive air showers (EAS). Numerous hadrons are produced in these cascades, among which mesons such as $\pi/K$ can decay into muons. The energies of these muons span from the GeV scale to TeV and beyond [1]. Over the past decade, ground-based array experiments have reported a notable deficit in simulated muons from EAS induced by high-energy cosmic rays, compared with experimental measurements [2]. This discrepancy, commonly referred to as the *muon puzzle*, reflects the limited understanding of hadronic interactions in EAS and the corresponding muon production mechanisms [3].

In ground-based experiments, the detected muons typically have GeV-scale energies and are produced during the final stages of shower development. By contrast, for underground detectors, the rock overburden absorbs the vast majority of low-energy muons, allowing only TeV-scale muons to penetrate and generate signals. These high-energy muons are generally produced in the early stages of the air shower, carrying a significant fraction of the primary cosmic-ray energy. They also exhibit small transverse momenta and thus provide critical information on hadronic interactions in the far-forward region. Consequently, underground experiments open a unique window to probe muon production mechanisms in EAS and to provide additional constraints for resolving the *muon puzzle*.

This phenomenon has also been investigated with underwater neutrino telescopes. For example, KM3NeT, which detects muons from sub-TeV to multi-TeV energies, has reported atmospheric muon fluxes exceeding model predictions, echoing the findings of ground-based studies [4]. Similarly, in ground-based spectrometer experiments such as BESS and L3, the measured muon flux at sub-TeV energies shows comparable discrepancies with theoretical expectations [5–7]. In this work, we investigate energetic muons produced in EAS at the China Jinping Underground Laboratory (CJPL), where a vertical rock overburden of 2,400 meters provides an ideal environment for studying cosmic muons above 3 TeV [8]. The underground muon flux is precisely measured with a 1-ton prototype detector of the Jinping Neutrino Experiment (JNE) in CJPL-I (the first phase of CJPL) [9]. Furthermore, we establish a comprehensive GEANT4-based simulation framework to predict the underground muon flux and compare it with the measurement, thereby contributing new insights into muon production in EAS.

## 2. Experiment

Located in the Jinping Mountains of Sichuan Province, China, with a vertical rock overburden of about 2400 meters, CJPL is the deepest and largest underground laboratory in the world. This unparalleled depth provides exceptional shielding from cosmic rays, making it an ideal site for rare-event searches such as dark matter and neutrinos. A variety of physics experiments are currently operating at CJPL. Among them, the Jinping Neutrino Experiment (JNE), constructed in Hall D2 of CJPL-II (the second phase of CJPL), is dedicated to MeV-scale neutrino studies, including solar, geo-, and supernova neutrinos, as well as neutrinoless double beta decay [10].

The one-ton detector, operational since 2017, was originally built as a prototype of JNE, primarily for technical validation and in-situ background measurements. In this work, we employ this detector to measure underground muons. The detector consists mainly of an acrylic vessel filled with liquid scintillator, surrounded by thirty inward-facing photomultiplier tubes (PMTs) that serve as highly sensitive photon sensors. When a muon traverses the target volume, it generates copious scintillation photons along its track. After propagation, these photons are collected by the PMTs, whose signals are digitized as waveforms by the electronic readout system for subsequent reconstruction. Further details about the detector can be found in Refs. [9, 11].

## 3. Simulation

We develop a comprehensive framework to simulate the detector response to underground muons, based on several widely used packages. The simulation procedure is divided into three steps: muon production in EAS, muon propagation through the mountain, and muon interactions in the detector.

Muon production in EAS is simulated using the Matrix Cascade Equation (MCEq) package [12, 13], which numerically solves the cascade equations governing air-shower development and computes the surface muon flux distributions $\phi_s(E, \theta)$. The inputs to this calculation are hadronic interaction models and the cosmic-ray energy spectra of all mass components. In this study, hadronic interactions are described by post-LHC models including SIBYLL-2.3d, EPOS-LHC, and QGSJET-II-04 [14–16]. The cosmic-ray spectra are taken from the Global Spline Fit (GSF) model, which is constrained by cosmic-ray measurements from both space- and ground-based detectors [17].

Muon propagation in the mountain is simulated with the Geant4 package [18, 19]. For TeV-scale muons, the dominant energy losses in rock arise from ionization and radiative processes, which are modeled using the standard electromagnetic physics list in Geant4. The mountain is realistically modeled with the surrounding terrain and the rock composition (marble, density 2.8 g/cm$^3$) [20, 21]. The surface flux distribution is used to sample incident muon events. From this simulation, the muon survival probability after traversing the rock, $P(E, \theta, \varphi)$, is obtained. Convolution of $\phi_s(E, \theta)$ with $P(E, \theta, \varphi)$ yields the underground muon flux distribution $\phi_u(\theta, \varphi)$. The simulation indicates that muons reaching CJPL have surface energies exceeding 3 TeV. The corresponding primary cosmic-ray energies are estimated to range from tens of TeV to above the PeV scale, with an average of about 0.4 PeV, as shown in Fig. 1.

The detector simulation of underground muons is also performed with Geant4, incorporating the detailed detector geometry. Underground muons are sampled from $\phi_u(\theta, \varphi)$ and generated on the walls of the experimental hall. The full detector response, including muon interactions, optical photon propagation, PMT detection, and electronic readout, is obtained in the same data format as the experimental measurements. Reconstruction algorithms for both deposited energy and direction are then applied to the simulated events, ensuring consistency with the data. Further details of the detector simulation are provided in Ref. [11].

## 4. Measurement

We analyze the full data set collected by the detector from July 31, 2017 to March 27, 2024, corresponding to an effective live time of 1338.6 days after data-quality checks. Two characteristic

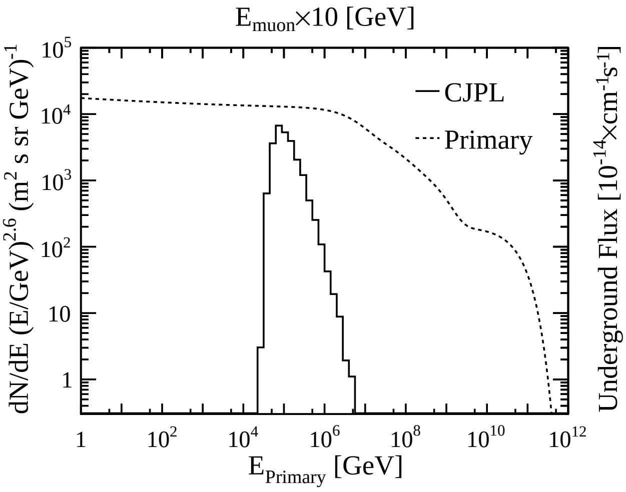


**Figure 1:** Surface energy distributions of muons arriving at CJPL-I, together with the primary cosmic-ray energy spectrum parameterized in Ref. [22]. The hadronic interaction model SIBYLL-2.3d is adopted to describe the EAS development. For comparison with primary cosmic rays, the muon energy is scaled by a factor as discussed in Ref. [13].

variables are extracted from the waveforms: the number of peaks, and the ratio of maximum charge to total charge. These variables are used to reject electronic noise and spontaneous light emissions from the PMTs, respectively, with negligible efficiency loss. By further requiring the visible energy to exceed 90 MeV, a total of 547 muon events are selected. The selection criteria are validated using simulation samples, and the corresponding efficiencies are also derived, as described in Ref. [11].

The deposited energy and direction of the muon events are reconstructed from the recorded PMT waveforms. The integrated charge of each PMT, after calibration, is summed to determine the total deposited energy. Natural radioactivity events in the detector are employed to calibrate the energy scale. Muon directions are reconstructed using a template-matching method, where templates generated by simulation are compared with the data. The template that yields the most similar detector response is chosen to infer the muon direction. Further details of these reconstruction methods can be found in Ref. [11, 23].

The underground muon flux is then determined as

$$\phi_\mu = \frac{N_{\text{total}}}{T \times S} = \frac{N_\mu}{\varepsilon \times S \times T}, \tag{1}$$

where $N_\mu$ is the number of selected candidates in the data, $T$ is the effective DAQ time, $\varepsilon$ is the trigger efficiency, and $S$ is the equivalent projection area of the experimental hall. The dominant systematic uncertainties in this measurement arise from the energy scale and the detector geometry implemented in the simulation, and are estimated to be 2.2% based on simulation studies. Consequently, the total muon flux at CJPL-I is measured to be $(3.54 \pm 0.15_{\text{stat.}} \pm 0.08_{\text{syst.}}) \times 10^{-10}$ cm$^{-2}$s$^{-1}$.

## 5. Comparison and Discussion

The underground muon flux at CJPL can be predicted using the simulation framework described in the previous section. In these predictions, the dominant sources of uncertainty arise from the

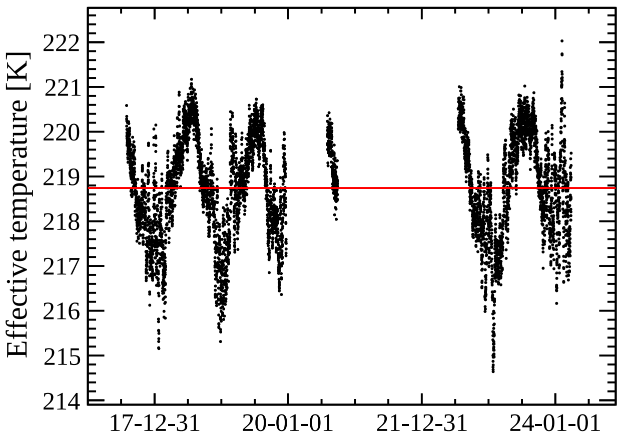


**Figure 2:** Effective atmospheric temperatures relevant for muon production in air showers during the data-taking period. The red line indicates the average value.

detector position and seasonal variations. Due to the complex terrain above the laboratory, the detector position cannot be precisely determined, which introduces an uncertainty into the muon flux prediction. To address this, a data-driven method is employed: the angular distribution of muons in data is compared with that from simulation to constrain the detector position and quantify the associated uncertainty, which is evaluated to be 1.6%.

In addition, the data collection period is not evenly distributed across the seasons, while the EAS calculations assume a year-averaged atmospheric model. Seasonal variations of the atmosphere can therefore contribute to the prediction uncertainty. The effective atmospheric temperatures during the data-taking period are calculated following Ref. [24], as shown in Fig. 2. The standard deviation of the effective temperatures over the data-taking period is used to estimate this effect, resulting in an additional flux uncertainty of 0.5%.

Then, we compare the underground muon flux at CJPL between measurement and prediction, as shown in Fig. 3. The measured flux exhibits an excess of about 40% relative to the predictions across all three hadronic interaction models, with no observable angular dependence. These discrepancies suggest that the models do not accurately describe the initial interactions in EAS, particularly meson production. A moderate enhancement of kaon and charmed-meson production in the early stages of EAS could account for the observed differences. Compared with the abundant pions produced in EAS, kaons and charmed mesons are more likely to decay into muons rather than undergo further interactions, thereby increasing the muon yield. Alternatively, if the hadronic models are assumed to be valid in this energy range, the discrepancies could instead imply a lighter mass composition of primary cosmic rays in the corresponding energy region.

## 6. Summary and Outlook

In summary, we have carried out the first investigation of muon production in air showers at CJPL using 1338.6 live days of data collected with the 1-ton prototype detector of JNE. Our

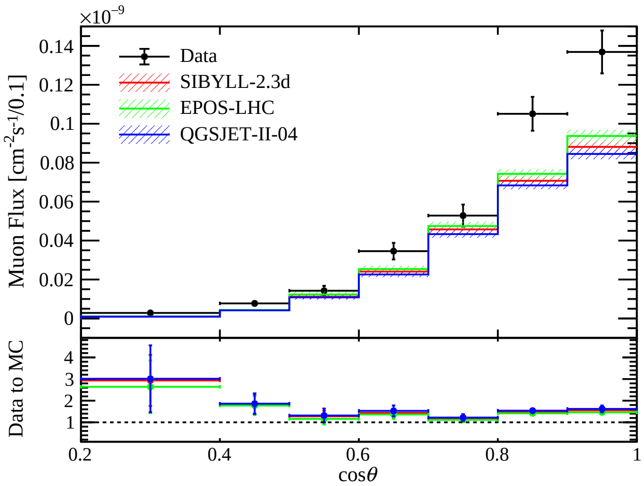


**Figure 3:** Comparison of the underground muon flux at CJPL-I between data and predictions based on post-LHC models at different zenith angles. In the top panel, measurement uncertainties are shown as error bars, while prediction uncertainties are indicated by dashed bands. In the bottom panel, both measurement and prediction uncertainties are combined and displayed as error bars.

measurement shows an approximately 40% excess in the muon flux compared with theoretical predictions. This discrepancy may be explained by a moderate enhancement in kaon production during the initial hadronic interactions of EAS. Expanding this detection technique to an array of underground detectors would allow precise reconstruction of shower vertices and extraction of more detailed information on cosmic rays and EAS. Looking ahead, the ongoing 500-ton detector of the Jinping Neutrino Experiment will record large samples of high-energy muon events, enabling further studies to help clarify these discrepancies.

## References

[1] T. K. Gaisser, R. Engel, and E. Resconi, *Cosmic Rays and Particle Physics: 2nd Edition* (Cambridge University Press, 2016).

[2] A. Aab *et al.* (Pierre Auger), Phys. Rev. Lett. **117**, 192001 (2016).

[3] J. Albrecht *et al.*, Astrophys. Space Sci. **367**, 27 (2022).

[4] S. Aiello *et al.* (KM3NeT), Eur. Phys. J. C **84**, 696 (2024).

[5] S. Haino *et al.*, Phys. Lett. B **594**, 35 (2004).

[6] P. Achard *et al.* (L3), Phys. Lett. B **598**, 15 (2004).

[7] A. Fedynitch, W. Woodley, and M.-C. Piro, Astrophys. J. **928**, 27 (2022).

[8] J.-P. Cheng *et al.*, Ann. Rev. Nucl. Part. Sci. **67**, 231 (2017).

[9] Y. Wu *et al.*, Nucl. Instrum. Meth. A **1054**, 168400 (2023).

[10] J. F. Beacom *et al.* (JNE), Chin. Phys. C **41**, 023002 (2017).

[11] X. Zhang *et al.* (JNE), Phys. Rev. D **110**, 112017 (2024).

[12] A. Fedynitch, R. Engel, T. K. Gaisser, F. Riehn, and T. Stanev, EPJ Web Conf. **99**, 08001 (2015).

[13] A. Fedynitch, F. Riehn, R. Engel, T. K. Gaisser, and T. Stanev, Phys. Rev. D **100**, 103018 (2019).

[14] F. Riehn, R. Engel, A. Fedynitch, T. K. Gaisser, and T. Stanev, Phys. Rev. D **102**, 063002 (2020).

[15] T. Pierog, I. Karpenko, J. M. Katzy, E. Yatsenko, and K. Werner, Phys. Rev. C **92**, 034906 (2015).

[16] S. Ostapchenko, Phys. Rev. D **83**, 014018 (2011).

[17] H. P. Dembinski, R. Engel, A. Fedynitch, T. Gaisser, F. Riehn, and T. Stanev, PoS **ICRC2017**, 533 (2018).

[18] S. Agostinelli *et al.* (GEANT4), Nucl. Instrum. Meth. A **506**, 250 (2003).

[19] J. Allison *et al.*, IEEE Trans. Nucl. Sci. **53**, 270 (2006).

[20] Z. Z. Liu *et al.* (CDEX), Phys. Rev. D **105**, 052005 (2022).

[21] M. Zheng, S. Li, Z. Feng, H. Xu, and Y. Xiao, International Journal of Mining Science and Technology **34**, 179 (2024).

[22] T. K. Gaisser, Astropart. Phys. **35**, 801 (2012), arXiv:1111.6675 [astro-ph.HE] .

[23] Z. Guo *et al.* (JNE), Chin. Phys. C **45**, 025001 (2021).

[24] E. W. Grashorn, J. K. de Jong, M. C. Goodman, A. Habig, M. L. Marshak, S. Mufson, S. Osprey, and P. Schreiner, Astropart. Phys. **33**, 140 (2010).